Tellus (1978), *30*, 32–54

Initialization with the data assimilation method

By K. MIYAKODA, R. F. STRICKLER and J. CHLUDZINSKI, *Geophysical Fluid Dynamics Laboratory/NOAA, Princeton University, Princeton, New Jersey 08540, U.S.A.*

(Manuscript received January 10; in final form June 15, 1977)

ABSTRACT

The initial conditions generated by a data assimilation technique with a general circulation model were evaluated. Two types of dynamic initialization, i.e., "the forward adjustment" and "the forward-backward adjustment", were tested using the real data produced by the NMC objective analysis. The degree of balance in the initial condition was examined in terms of the smoothness in the development of the rate of precipitation, angular momentum, and kinetic energy during the starting period of the prediction. The quality of the initialization was, however, appraised by the performance of the subsequent prediction. For the forward adjustment, various types of schemes of data insertion were studied with regard to the amount of shock produced and the degree of faithfulness of the injected data. In dealing with forward-backward processes, one difficult problem is how to design a reversible algorithm. An approximate method is presented for maintaining the reversibility in a system which includes kinetic energy dissipation, radiation, and the moist heating. In addition, the question is discussed as to which physical processes of the model must be included for the forward-backward initialization. It is found that the dynamic initialization using the forward-backward data assimilation produces predictions that are, in some ways, better than those from the static or conventional initialization. However, for the forward data assimilation the predictions are consistently worse than those from the static initialization.

1. Introduction

One intriguing and yet serious problem encountered in numerical weather prediction is that the forecast error develops rather rapidly and appreciably at the initial time, i.e., within one day. The question is whether this fast error growth is due to inappropriate initial conditions or the inadequacy of the forecast model. The former may be further classified as to whether the imperfect initial condition is due to inaccuracies in the analysis or due to imperfect initialization. The analysis and the initialization are mutually related, and a clear-cut distinction is sometimes difficult. Yet in this paper we shall confine our discussion to the initialization as much as possible.

The initialization referred to here is the process of making the set of adjusted variables required for a marching integration where the variables are mutually balanced within the dynamical framework of a particular prediction model, keeping some dominant variables the same as the original observations or analysis and modifying, if necessary, other less dominant variables. A satisfactory initial condition, therefore, (1) provides a smooth transition of the predicted state from the initial to the model's asymptotic level, and (2) guarantees that the subsequent forecasts will be accurate. Perhaps the second requirement is more important than the first.

There have been two basic approaches for obtaining the initial condition, which Bengtsson (1975, see page 58) has called *static initialization* and *dynamical initialization*. Examples of the former are (a) the method based on the balance equation and ω-equation, and (b) multivariate optimum interpolation analysis. The dynamical initialization uses the non-stationary dynamic equations one way or another. Undoubtedly a really smooth start of forecast can be achieved by dynamical initialization, in which the prediction model is involved for the construction of the initial state. In this approach, the data for the dominant variables are inserted into the prognostic equations, and thereby the balanced condition is achieved. Although the problem is essentially related to the classical geostrophic adjustment theory (for example, see Monin and Obukhov, 1959), its application to initialization required a great deal of additional research.

The aim of this paper is to discuss the practicality of useful dynamical initialization schemes and whether they can really yield higher quality forecasts than the conventional initialization schemes.

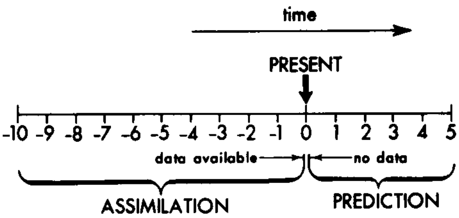

Fig. 1. The data assimilation and the prediction.

2. Set-up of problem and preparation of data

2.1 *Problem*

Let us assume that the data for Z (geopotential height) and T (temperature) are given at all gridpoints or some selected gridpoints on a regular net. The problem is how to construct a complete set of initial conditions from these data for a particular prediction model. The initial condition consists of all necessary meteorological variables such as $\mathbb{V}$ (horizontal wind vector), ω (vertical pressure velocity), T (temperature), p_s (surface pressure) and q (mixing ratio of water vapor), and they should be mutually well adjusted under the dynamical constraints imposed by the model. The adjustment in the normal general circulation model concerns a number of dynamical relations such as hydrostatic and geostrophic balance and other constraints related to the condensation of water vapor, boundary layer drag, and radiational cooling/-heating.

To begin with, it may be convenient to consider a schematic diagram of the time coordinate (Fig. 1), extending from the past through the present to the future. The objective is to obtain initialized data at the "present" time, making use of the data of Z and T in the past and the present. The original data for Z and T are provided in the form of two-dimensional maps for the mandatory pressure levels, which could be a result of either an objective analysis or a four-dimensional analysis (so-called Level III data). In practice, the operational objective analysis at NMC (National Meteorological Center, Washington, D.C.) was used. The values of Z and T (and q, analyzed by our objective scheme) at 12 h intervals, i.e., 00 and 12 GMT existed at the Cartesian coordinate points of the NMC grid with a mesh size of 381 km at 60° N on the hemispheric stereographic projection maps on the twelve pressure levels, 10, 30, 50, 100, 150, 200, 250, 300, 500, 700, 850 and 1000 mb. In reality, however, the stratospheric data at 10, 30, 50 and 100 mb were only available every 24 h, i.e., 12 GMT, so that the maps for 00 GMT were produced by time interpolation.

2.2 *The prediction model*

The model used was the GFDL (Geophysical Fluid Dynamics Laboratory) hemispheric, general circulation model with nine vertical levels and $N = 40$ horizontal resolution, where N is the number of gridpoints between the pole and the equator, and its horizontal grid size is about 270 km at the middle latitude (see Manabe et al., 1965; Miyakoda, 1973). The model uses the σ-coordinate system and has topography. The nine sigma levels are: .0089, .0741, .1886, .3361, .5000, .6639, .8114, .9259 and .9911. It includes all of the usual physical processes such as radiation, land–sea contrast, water vapor processes, surface drag and vertical and horizontal subgrid-scale diffusion.

2.3. *Pre-processing of the data*

Let us mention here the pre-processing of the data, which was done on the stereographic grid using the conventional initialization scheme (see Haltiner, 1971). Using Z and T with the aid of q, we first obtained the three-dimensional distributions of $\mathbb{V}$, ω and p_s.

The wind vector is divided into the rotational component $\mathbb{V}_\psi$ and the divergent component $\mathbb{V}_\chi$, and is written as

$$\mathbb{V} = \mathbb{V}_\psi + \mathbb{V}_\chi,$$
$$\mathbb{V}_\psi = \nabla \times \psi, \quad \text{and} \quad \mathbb{V}_\chi = \nabla \chi \tag{2.1}$$

where ∇ is the nabla del operator, ψ is the stream function and χ is the velocity potential.

The rotational component V_ψ is obtained from the so-called "balance equation", which is written:

$$2(\psi_{xy}^2 - \psi_{xx}\psi_{xx}) - f(\nabla^2 \phi) - (f_x\psi_x + f_y\psi_y) + \nabla^2 \phi = 0,$$

where $\phi = gz$, g is the acceleration of gravity, f is the Coriolis parameter, and only here the subscripts denote the derivatives. Given ϕ on the pressure surfaces, this ψ equation may be solved. The divergent component V_χ is derived from the "ω-equation", which is written: $\nabla^2(\omega\Lambda) + f^2(\partial^2\omega/\partial p^2) + F = 0$, where p is the vertical coordinate, $\omega \equiv dp/dt$, F is the forcing function, which depends upon the known variables, and Λ is the static stability. The unknown ω is solved from the elliptic equation. The velocity potential x is given by the equation: $(\partial\omega/\partial p) + \nabla^2\chi = 0$. Thus the total wind vector $V = V_\psi + V_\chi$ is obtained. The calculation for V was carried out for the horizontal domain of 5025 gridpoints at the twelve vertical pressure levels.

The surface pressure p_s is derived from the hydrostatic equation and the equation of state in such a way as to be consistent with the model's topographical height Z_*. A set of variables obtained in this way will be used as an initial condition, although our whole objective in this paper is to design a new initialization which is better than this conventional initialization.

2.4. *The insertion data*

In order to carry out the insertion process in the four-dimensional analysis, the observation network was simulated as a subset of the model's 5025 gridpoints in the hemispheric domain. The data at these observation stations will be inserted into the prediction model and the variables at the rest of the gridpoints are allowed to retain their forecast value. In this study, the station points were defined as the gridpoints nearest to the locations in the operational WWW (World Weather Watch) network. This is because we thought it reasonable to assume first that the data at these points are more reliable than at other points.

We used three kinds of network; they are the *crude*, the *refined* and the *very refined* networks, which are referred to as A, B and C networks (see Fig. 2). The A-network is the simulation of observation stations which was actually in operation at the time of November, 1969 (Basic Data Set experiment period); the B-network is the stations envisaged to be implemented at FGGE, 1978; the C-network consists of every third gridpoint (in each dimension) out of the total hemispheric net superimposed on the B-network.

The meteorological data were taken from the data set based on operational NMC analysis at these stations at 12 h intervals. The wind and temperature at the mandatory pressure surfaces of the upper air stations, and the surface pressure at the surface stations were prepared. In most of our experiments, we used the 2 h interval data for the insertion, which were derived by a linear interpolation from the 12 h interval data. The wind and temperature data at pressure levels were then interpolated to the sigma-surfaces.

The data in the planetary boundary layer, i.e., levels 8 and 9, were not inserted, because the proper temperatures in this layer were not obtained in the original analysis. In a preliminary study using the hypothetical "identical twin" data test, it was demonstrated that the solution of the initialization adjusts itself in a reasonable manner even if no data were injected in this layer.

2.5. *The forced adjustment*

The data assimilation started from an initial condition which was prepared by the conventional initialization method described earlier. The generation of gravity waves was not particularly great. Two versions of the adjustment were tested. One is referred to as the "forward adjustment" (see Fig. 3), in which the data are inserted during forward marching calculation. The second is the "forward-backward adjustment" (Fig. 4) in which the insertion was performed during the forecast as well as the hindcast cycles (Bengtsson, 1975).

In general, whenever new data are inserted in a model, they normally create a discontinuity with the current model solution. As has been extensively investigated, the fluid's dynamical characteristics enable it to remove this discontinuity in such a way as to maintain a state of approximate geostrophic balance. In this adjustment process, inertia-gravity waves are generated and dispersed; this phenomenon may be described as the generation of "shocking". To reduce the shock effect, a number of techniques have been designed and are available. One treatment is to avoid the production of discontinuity by the *repeated insertion of 2 h interpolated data* each time step (Mesinger, 1972; Gordon and Lusen, personal communication), *the weighted average of inserted data and the model solution* (Mesinger, 1972), *optimum interpolation* (Bengtsson and Gustavsson, 1971), and *Newtonian*

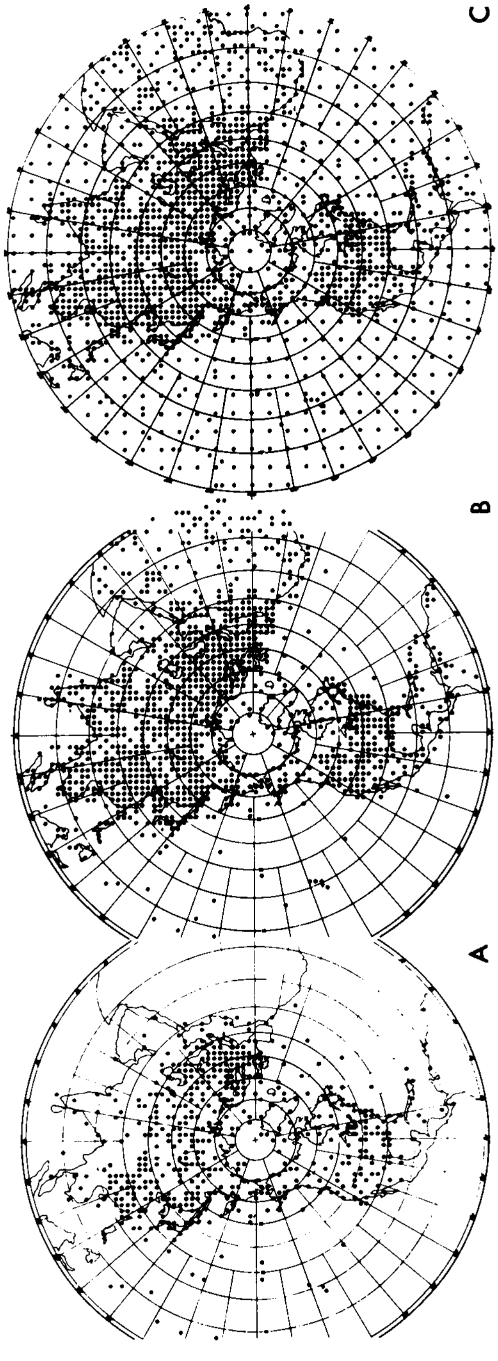

Fig. 2. The insertion gridpoints. A, B and C networks.

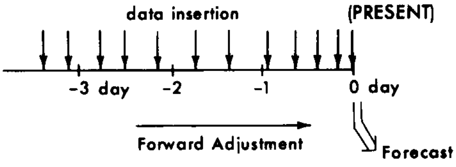

Fig. 3. Schematic diagram of forward adjustment.

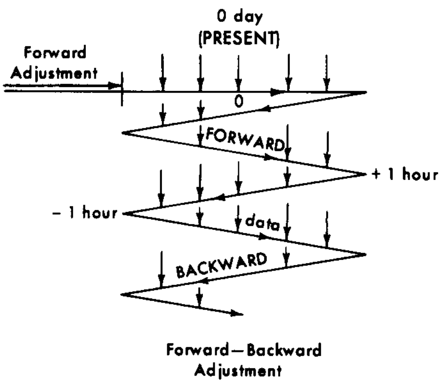

Fig. 4. Schematic diagram of forward-backward adjustment.

damping (Anthes, 1974; Davies and Turner, 1976). The other treatment is to damp the gravity waves, if noise is produced, by *Euler-backward* damping (Matsuno, 1966; Kurihara, 1965; Miyakoda and Moyer, 1968), *time filtering* (Asselin, 1972; Rutherford and Asselin, 1972), *divergence damping* (Sadourny, 1972; Talagrand, 1972), or *vorticity damping* (Simmonds, 1976).

In the forward adjustment of our test, the Euler-backward method was used intermittently, whereas in the "forward-backward adjustment", the Euler-backward method was used continuously. The weighted average (Mesinger, 1972) was also used in some experiments. The formula is,

$$\xi_{\text{insert}} = \gamma\xi_{\text{input}} + (1-\gamma)\,\xi_{\text{model}}, \tag{2.2}$$

where ξ is an arbitrary variable, "input" means the original data value, "model" is the current model solution and "insert" is the data actually inserted. If $\gamma = 1$, the model solution is completely replaced by the input data. When γ is far less than 1, the "shocking" diminishes appreciably.

2.6. *The data cases*

We tested two real data cases. One case is 00 GMT January 4, 1966, as the 0th day, which gave the worst forecast among the twelve winter cases (Miyakoda et al., 1972), and the second case is 12 GMT March 14, 1965.

3. Forward adjustment

3.1. *Various experiments*

A number of experiments were conducted to test the adjustment and data assimilation in the forward injection (Charney et al., 1969). Among them, we will discuss only nine experiments below, i.e., Exper. a, b, k, l, m, n, p, q and R (see Table 1).

In all but two experiments, the assimilation started at -5 day with the conventional initial condition; the exceptions are Exper. l, which started at -10 day, and Exper. R at 0 day. Exper. R is not an assimilation but the prediction calculation starting from the conventional

Table 1. *Experiments of forward adjustment*

Exper.	Insertion data	Insertion method	Data density	Weight	Remarks
a	T, p_s (a, b)	contin.	A		
b		contin.	A	$\gamma_1 = 1.0$, $\gamma_2 = 0.15$	
k	T, V_ψ, p_s (k, l, m, n, p)	12 h interv.	A		
l		contin.	A		
m		contin.	A	$\gamma_1 = 0.6$, $\gamma_2 = 0.15$	
n		contin.	B	$\gamma_1 = 1.0$ (n, p)	T in PBL
p		contin.	C	$\gamma_2 = 0.15$ (n, p)	T in PBL, no data in Tropics
q	$T, V_{\psi+\chi}, p_s$	contin.	B	$\gamma_1 = 1.0$, $\gamma_2 = 0.15$	T in PBL

initialization, which is used for reference. The data were injected every timestep except that, in Exper. k, the insertion was made every twelve hours (at 12 h intervals, the same data was entered in the model every timestep for 2 h periods).

The Euler-backward damping was applied intermittently, except in Exper. n, and q, where the damping was used continuously during the last day of data assimilation. Imitating optimum interpolation schemes (Blumen, 1975), not only the observing station itself but also the surrounding points were taken for the insertion data in some experiments. γ_1 is the weighting factor for station data and γ_2 is that for the four adjacent gridpoints. In Exper. n, p and q the refined networks in Fig. 2B and 2C were used, and the temperature data were inserted at all levels including level 8 and 9.

3.2. *The spin-up*

Let us first look at some features of the time variation of the assimilation process and the transition from the assimilation to prediction. Figs. 5, 6, and 7 show the evolution curves of some selected variables of the model solutions throughout the time coordinate of past, present and future. In these diagrams, three curves are shown (Exper. l, k and a) for the assimilation part and two curves (Exper. l and R) for the prediction part.

Fig. 5 is $\overline{\omega^2}$ averaged three-dimensionally over the whole hemisphere. This variable is a good measure of the intensity of gravity waves and, accordingly, of the degree of the "shocking". In Exper. 1, the variation of $\overline{\omega^2}$ is relatively smooth, whereas the curve for Exper. k has sharp peaks every 12 hours. This implies that the large

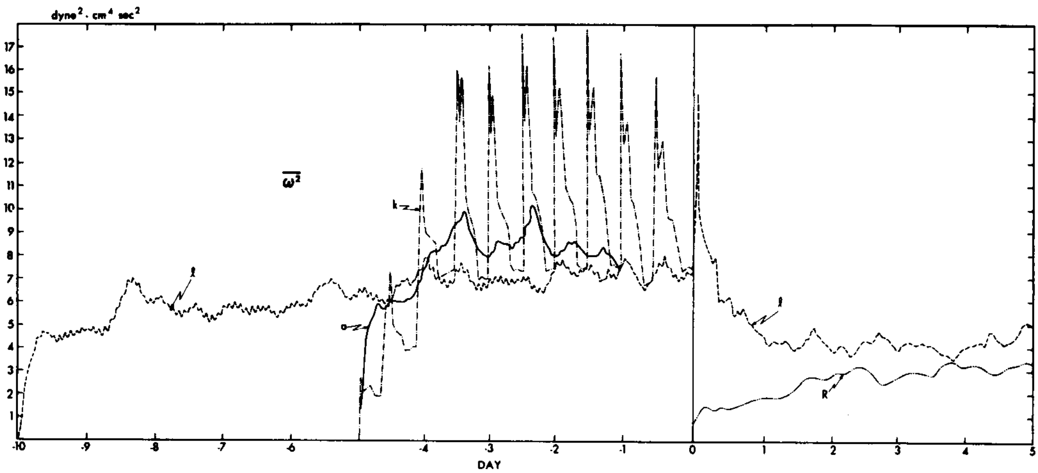

Fig. 5. $\overline{\omega^2}$ curves in forward adjustment and the subsequent prediction.

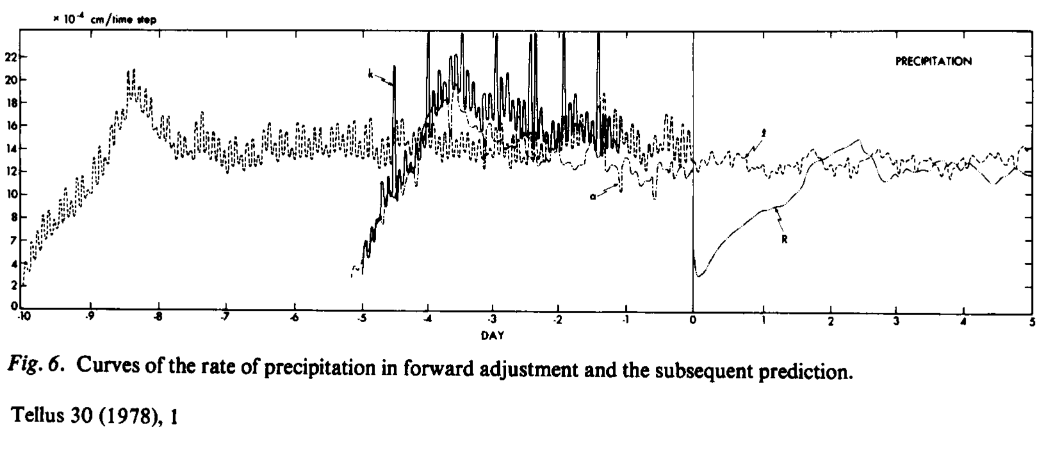

Fig. 6. Curves of the rate of precipitation in forward adjustment and the subsequent prediction.

"shocks" were created every time the data was inserted, suggesting that intermittent injection is less favorable than the continuous injection from the standpoint of noise level. Exper. a has a somewhat large value of $\overline{\omega^2}$ compared with Exper. l, in spite of the fact that this experiment used only the temperature and the surface pressure for the insertion. After the marching calculation moved into the forecast stage, $\overline{\omega^2}$ for Exper. l first increased for a short while, then decreased quickly and approached the same level of Exper. R after about 3 days.

One of the real advantages of dynamical initialization is demonstrated in the evolution of the hemispheric-averaged rate of precipitation in Fig. 6. With conventional initial conditions (Exper. R), the precipitation curve normally starts at a small value (except the sharp drop at the initial time), then increases rather rapidly, reaching a peak at 2.5 days, and finally settles down at the 3rd day. The spin-up time is, therefore, 3 days. This trend is also seen in the curve of the data assimilation, although the spin-up time is distorted. (The increase in rate of rainfall is rapid.) We will come back to further details later.

The large contribution to the hemispheric-averaged rainfall comes from the equatorial region. In order to have tropical rain, the disturbances in the flow have to be properly generated first, and the water vapor field has to build up enough for cumulus convection to occur. These conditions seem to require a considerable spin-up time. In this regard, the initialization based on the data assimilation method such as Exper. 1 seems to give a favorable condition for the forecast in the tropics, compared with the conventional initial condition (Exper. R). Another point worthy of mention is the large amount of rainfall in the intermittent insertion (Exper. k). It is striking that the large shocks caused by the 12-h interval injection are accompanied by intense, intermittent precipitation, which is obviously spurious and is likely to adversely affect the mass and flow fields.

Fig. 7 contains the curves of absolute angular momentum averaged over the hemisphere,

$$\overline{M}_A^H = \iiint m_A \, dz \, dx \, dy / \iint dx \, dy,$$

$$M_A = a \cdot \cos \theta (u + a \cdot \cos \theta \cdot \Omega),$$

where u is the zonal component of wind, a the radius of the earth, Ω the angular velocity of the earth, and θ the latitude. In this case, the angular momentum appears to increase gradually from −9 day to +5 day. This was probably a natural trend for this particular interval of time. On the other hand, the angular momentum in Exper. R starts at a large value and the curves of Exper. R and l meet at 5 days. It is a known characteristic that the spin-up for the momentum takes a long time, i.e., about 10 days.

In this way, evidence has been presented to demonstrate that initial conditions derived using the assimilation method are well adjusted except for some oscillations of $\overline{\omega^2}$. However, the quality of a forecast produced from these initial conditions is another problem.

3.3. *The general tactic*

The verification of the initialization was made in terms of the assimilated results as well as the

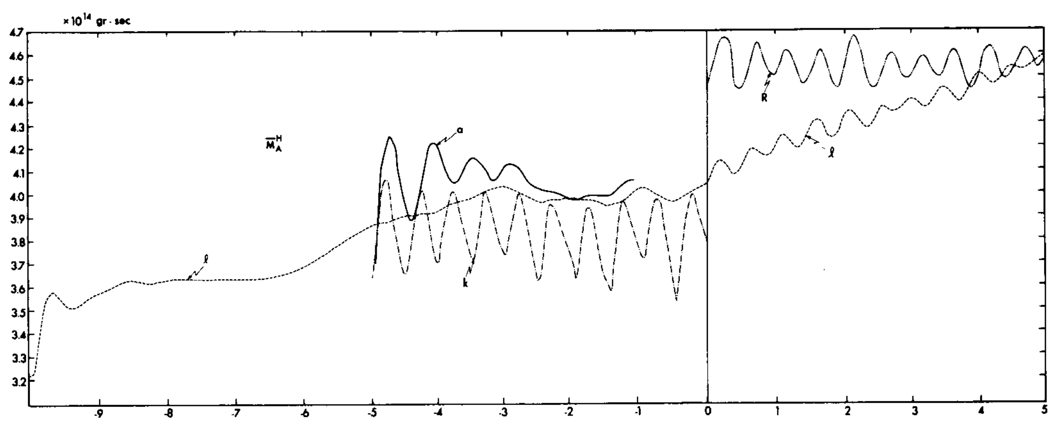

Fig. 7. Curves of the absolute angular momentum (M_A^H) in forward adjustment and the subsequent prediction.

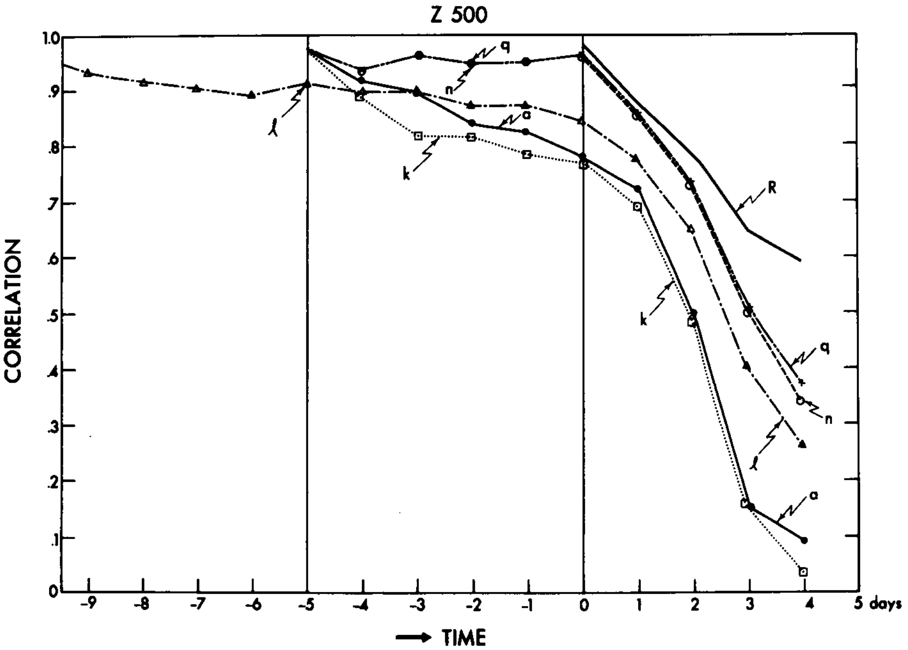

Fig. 8. Correlation coefficients of geopotential height at 500 mb.

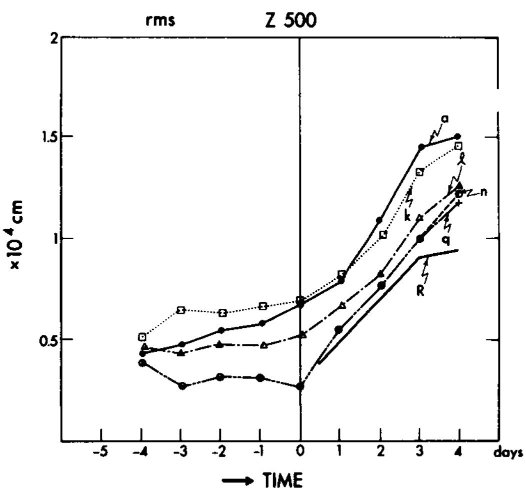

Fig. 9. Rms errors of geopotential height at 500 mb.

forecast results. Because our initialization is based on the inserted data of NMC analysis, it may not be logical to compare it with the NMC analysis. However, it is also true that the initialized result should reflect the inserted data and should not be too much different from the NMC analysis either. The verification based on the performance of forecasts is particularly important, because it is indeed our goal to obtain an initialization by the assimilation method that gives a better forecast than the reference forecast, Exper. R.

The degree of the similarity was assessed by the correlation coefficients of the anomaly of the assimilated (or forecast) geopotential heights from the monthly normal and the NMC counterpart as well as the root mean square (rms) of the difference of the geopotential heights between the assimilated (or forecast) analysis and the NMC analysis. The area of verification is north of 15° N.

3.4. *Comparison of the assimilated analyses*

Just for convenience, Exper. q, n, l, a, k and R are displayed in the verification diagrams. Figs. 8 and 9 show the verification scores comparing with the NMC analysis for 500 mb.

Let us focus our attention for a moment to the assimilation period. The similarities of the assimilated fields to the NMC fields were well preserved in some experiments over a long span of data insertion. For example, Exper. q, n and m are the group which have the most similarity, and Exper. l also shows resemblance, but to a lesser extent. On the other hand, in Exper. a, b and k, the similarity is generally much lower indicating that the model's influence is too large, or unfavorable

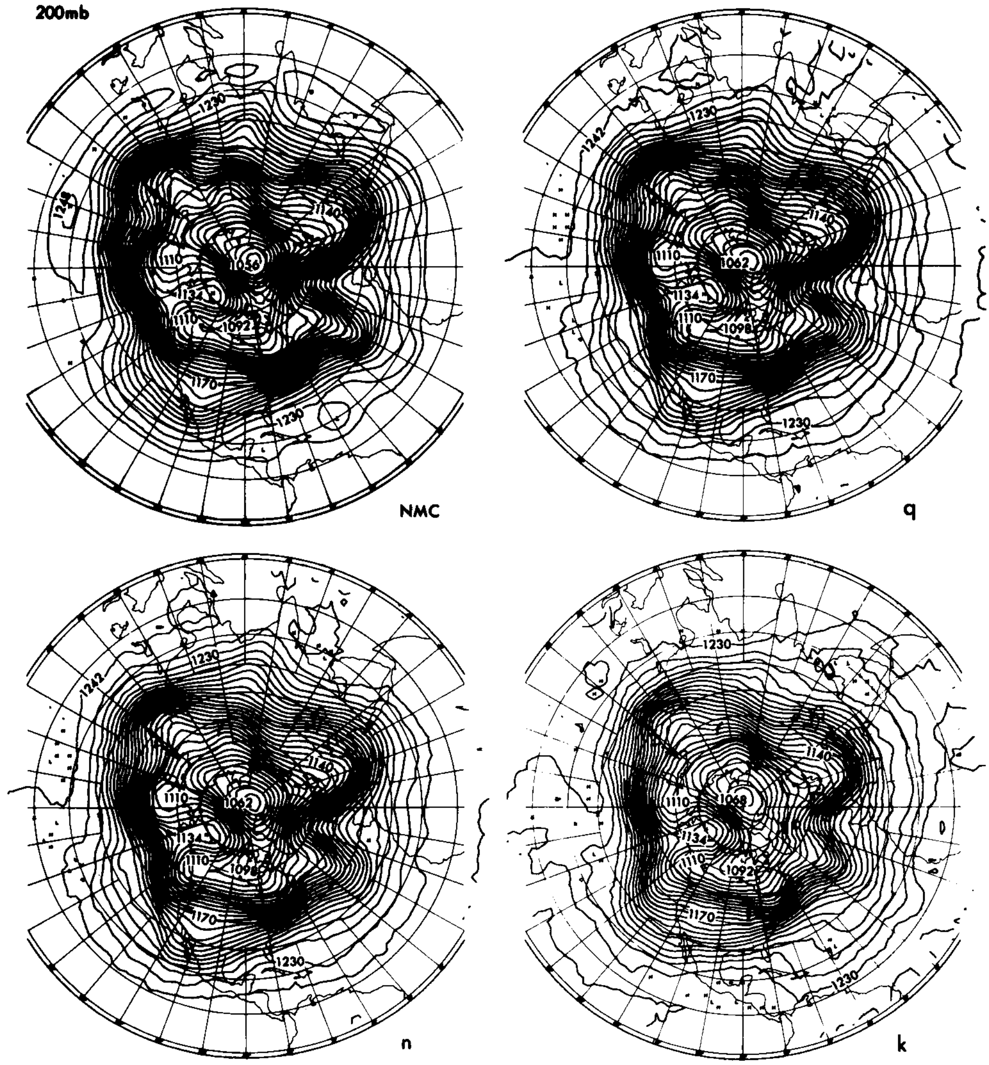

Fig. 10. Examples of the assimilated maps. The geopotential heights at 200 mb for NMC, Exper. k, n and q. The contour interval in 60 m.

hysteresis remains, or the gravity waves damaged the large scale flow. (The former point was mentioned also by Asselin, 1972; Gordon and Lusen, personal communication; Miyakoda et al, 1975. The latter by Morel et al., 1971; Bengtsson and Gustavsson, 1971; Gordon et al., 1972; Hayden, 1973; and Kistler and McPherson, 1975.) As seen in Exper. k, the intermittent insertion leads to an assimilated pattern which is less similar to the NMC pattern, even though wind data are also inserted. The insertion of large amounts of data improves the similarity, though ω^2 increases appreciably. This is indicated by comparisons of Exper. m vs n and Exper. a vs b (not shown). The weighting factors $\gamma_1 = 0.6$ and $\gamma_2 = 0.15$ gives the mixture of the insertion data and the model solution. Compared to $\gamma_1 = 1$ and $\gamma_2 = 0.15$, the above choice reduces the intensity of ω^2 appreciably (Blumen, 1975) without affecting the assimilated patterns very much.

At 1000 mb and 50 mb the distribution of verification scores for the assimilation period and

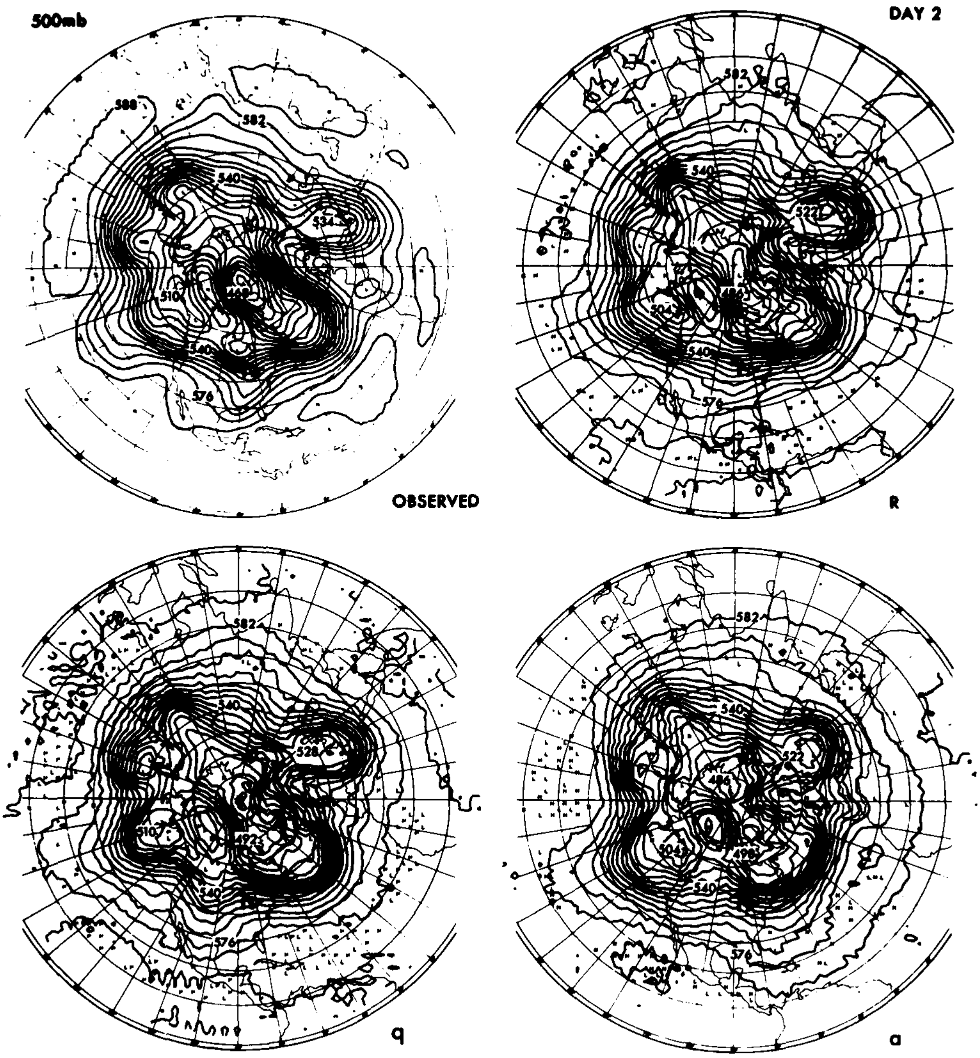

Fig. 11. The 2-day forecasts of the 500 mb geopotential height for Exper. a, q and R. The contour interval is 60 m.

the following forecast was similar to that at 500 mb. The results of the assimilated height fields at the end of the initialization are shown in Fig. 10. The differences of the assimilated maps vs the NMC maps are fairly small and subtle, so far as the geopotential height is concerned. However, this degree of subtleness is our concern, since it creates appreciable differences in the subsequent prediction.

If one observes these maps carefully, it may be noticed that Exper. q is closest to the NMC map, and next closest is Exper. n. Exper. k has noticeably over-smoothed and made shallow the troughs and ridges. In general, the assimilated maps have less intense gradient of the height contours.

3.5. *Comparison of the predicted maps*

Once the pure prediction phase begins at day 0, the similarity of the model solution to the NMC analysis decreases rapidly and appreciably (see Figs. 8 and 9). This is due primarily to predictability decay. Another crucial fact is that none of the assimilated initial conditions is superior to

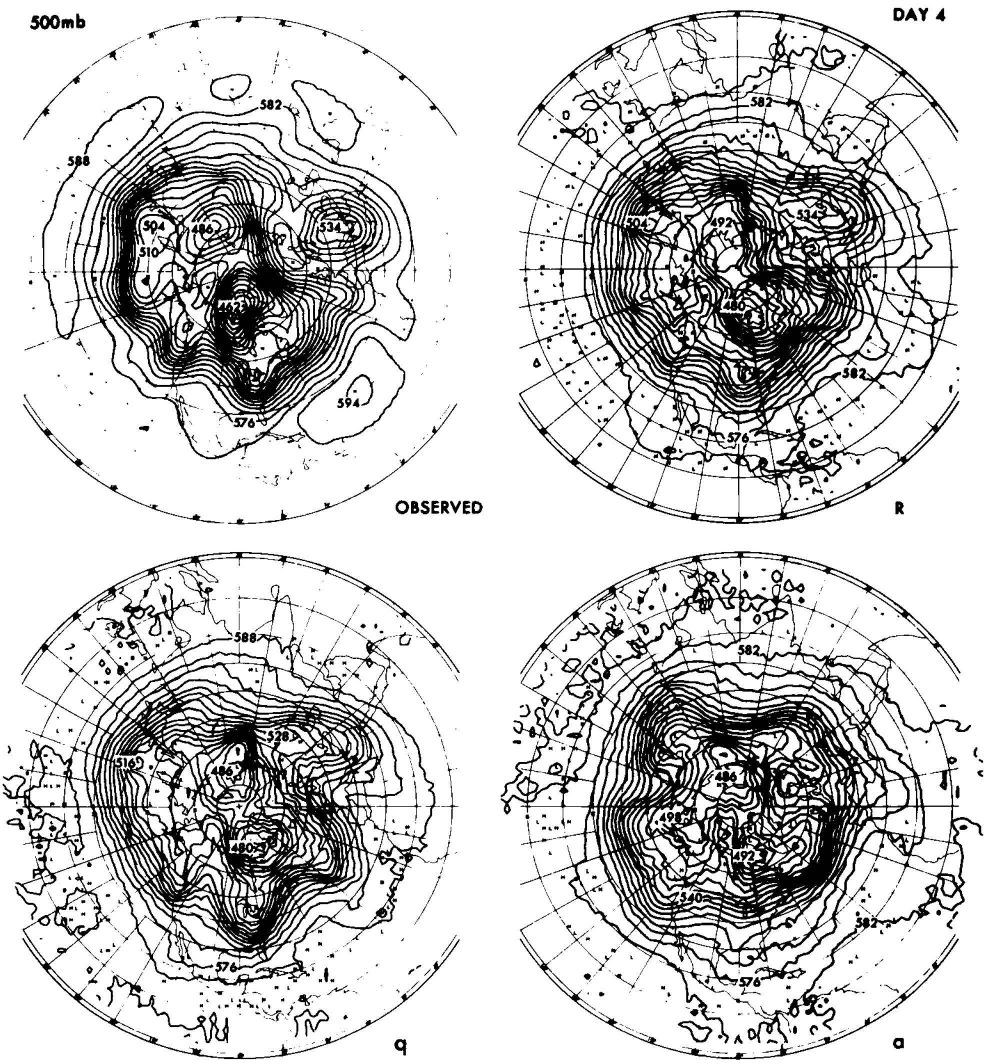

Fig. 12. The 4-day forecasts of the 500 mb geopotential height for Exper. a, q and R. The contour interval is 60 m.

Exper. R. It is also interesting to note that the performance of forecasts varies widely, depending on how the initial conditions were generated.

Exper. p, q, n and m give better forecasts than Exper. a, b and k. This trend is consistent with the degree of similarity of the assimilated fields to the NMC analysis. It suggests, therefore, that the wind data insertion, in addition to the temperature and surface pressure, yields better forecasts. The continuous insertion is more favorable than the intermittent insertion from this standpoint also.

Exper. q gives a slightly better forecast than Exper. n; this represents the benefit of utilizing the divergent component of wind. The increased insertion of data gives a better forecast, as indicated in Exper. p vs n, and n vs m, and also in Exper. b vs a (not shown).

In Figs. 11 and 12 the 2- and 4-day 500 mb height forecasts are compared with the observed (NMC) maps. In this display, Exper. q and a were selected, and Exper. R is also shown. Exper. q is the best forecast among those using the assimilated initial conditions, and Exper. a is one of the worst forecasts. However, R is still best overall in forecast performance, particularly in predicting the cut-off low over the Black Sea, whereas Exper. a is markedly poorer in every respect of performance.

The reason for the inferiority of the forecasts using the assimilated initial condition compared to Exper. R is not obvious. However, we make the following speculations. Evidently, the shortcomings of the forward adjustment method are: (a) the high level of noise, and (b) the excessive smoothness of the resulting flow fields. The first point seems to be less serious, if the noise is not excessive. We saw examples in which the synoptic scale flow fields are satisfactory despite the presence of small wiggles. We are particularly concerned about the second defect. It is an indication of insufficient intensity of wind shear near the jet streams. It is well known that the vorticity distribution is an extremely important factor for the dynamics of atmospheric flow more than just the advecting flow. Secondly, inspecting Figs. 11 and 12, we see that the forecast is poorest over the oceans. In the assimilated analyses of this study, insufficient data were inserted in the ocean areas. (As indicated by Exper. p which had higher verification scores at 500 and 50 mb than Exper. q (not shown), this defect was circumvented by inserting spatially denser data.) Concerning the drawback of the excessive smoothness, we speculate that the crudeness may come from the insufficient assimilation of the input data. Possibilities of improvement are (a) to let the model assimilate the inserted data more effectively, or (b) to use a model with the higher space resolution.

4. Forward-backward adjustment

In order to remove or alleviate the deficiencies in the forward adjustment, i.e., the insufficient assimilation and the high level of noise, it has been suggested by J. Smagorinsky (personal communication) that the injection of the data be iterative. Namely, instead of inserting a datum just once, the injection of the same information is repeated for many cycles at the same time level.

The idea was not quite new. In the initialization method, Miyakoda and Moyer (1968), Nitta and Hovermale (1969), and Nitta (1969a, 1969b) utilized this concept. Later Mesinger (1972) and Winninghoff (1973) developed this approach further, using the multi-time level forward-backward iteration in contrast to a single time level scheme. According to Mesinger, the multi-time-level method is more effective at producing rapid convergence of the solution. From the standpoint of the four-dimensional data assimilation, Morel et al. (1971) designed a forward-backward scheme, where the data are injected during both the 12 hour forecast and hindcast phases. Thus, Nitta and Hovermale (1969) and Morel et al. (1971) seem to provide an approach which is both simple and effective. In contrast to the original method of Miyakoda and Moyer, Nitta and Hovermale's method utilizes the primitive equations alone and no balance condition is assumed. This scheme has been favored in the meteorological community as seen in the examples of Temperton (1973, 1976), Gauntlett and Seaman (1974), Bourke (1974), Haltiner and McCollough (1975), Grant and Rivas (1975), Kanamitsu (1975) and Kiangi (1976). These papers have contributed not only to a better understanding of the problem but also to a sizeable speedup in the rate of assimilation. More recently Kistler and McPherson (1975) have investigated the scheme of forward-backward adjustment extensively for the purpose of the four-dimensional analysis and mentioned that even in this scheme restoration of the wind is important in accelerating convergence.

One of the difficulties in this method is, however, that if the prediction model becomes sophisticated and complicated, as is inevitably the case for general circulation models, the design of the forward-backward scheme is extremely difficult, if not impossible. For this reason, we have long avoided this approach and sought for an effective method within the framework of forward adjustment. As described in the previous section, however, we are now faced with the necessity of reconsidering this method.

There are a number of questions one has to answer in applying the forward-backward adjustment. One is whether all of the physical processes in the general circulation model should be included for the purpose of the initialization or the four-dimensional analysis. If necessary, one of the fundamental questions in the forward-backward calculation is whether or not reversibility can be maintained even if the model includes frictional terms, water vapor transfer, radiative transfer, heat released by condensation and other subgrid-scale processes. On the other hand, if it is not necessary to include all the physical processes, then which effects should be incorporated or excluded, and whether or not the effect can be treated in the forward-backward process.

4.1. *Reversible and irreversible processes*

Concerning the frictional term, for example, one of the authors was previously notified by J. R. Pasta (personal communication) that "the presence of a dissipation term does not change the mathematical reversibility if the positive dissipation is replaced by negative dissipation as necessary, although it may be physically unrealistic" (Bivines et al., 1972). Along the same line of thought, Miyakoda and Moyer (1968) demonstrated that the frictional term can be included in the forward-backward method of initialization.

During the backward, i.e., hindcast phase, the frictional term produces the amplification effect. Therefore, even small discrepancies of the solutions between the forward and the backward processes can be amplified to a large difference. For example, the round-off error can be the cause of irreversibility. But if the time span of the "round trip" is not so large, the growth of the irreversibility may be confined to a practically low level. Computationally, however, a problem still remains. The frictional term is often non-linear, and the frictional coefficient is a complex function of the prevailing flow and temperature field. With an iterative procedure, the reverse process can be solved in principle, but it is not practical. A reasonable method of treatment will be proposed in this paper. In short, unless the conversion of frictional dissipation into heat is taken into account, only the mechanical process of friction is completely reversible.

Some other subgrid-scale physical processes are more complicated and they could be irreversible. For example, in the small scale cumulus convection, the water vapor is transported upward, and then some portion is condensed, releasing heat. This process is irreversible. In the backward process the condensed water is evaporated and transported downward. It can be seen that the solution during the hindcast phase is not uniquely determined.

As will be discussed below, however, there may be an approximate but practically useful method to treat it. The principle of the scheme is the following. In the forward calculation, an inventory is kept as to the liberated heat and the converted water vapor; how much, at which gridpoint, at which level and what time level does the liberation and the conversion take place. Then in the backward calculation, the heating in the record is extracted and the depleted water vapor is returned to the atmosphere.

4.2. *Time differencing scheme for the forward and backward processes*

Let us first discuss the finite difference schemes for the reversible processes, taking a stepwise approach from a simple to a complicated system of equations. For simplicity, the equation of v will be omitted, where v is the wind component in y-direction.

A. Simple example including the vertical diffusion of momentum.

$$\frac{du}{dt} = fv - \frac{\partial \phi}{\partial x} + \frac{\partial}{\partial \sigma}\left(K \frac{\partial u}{\partial \sigma}\right), \tag{4.1}$$

$$\frac{dT}{dt} - \frac{RT}{C_p p_s \sigma}\,\omega = 0, \tag{4.2}$$

$$\frac{\partial p_s}{\partial t} + \nabla\cdot(\mathbb{V} p_s) + \frac{\partial \dot{\sigma} p_s}{\partial \sigma} = 0, \tag{4.3}$$

where u is the wind vector component for the x-direction, p_s is the surface pressure, σ is the σ-coordinate such that $p = p_s \cdot \sigma$, θ is the potential temperature (not latitude from here on), R is the gas constant, and

$$\frac{d}{dt} \equiv \frac{\partial}{\partial t} + u\frac{\partial}{\partial x} + v\frac{\partial}{\partial y} + \dot{\sigma}\frac{\partial}{\partial \sigma}, \tag{4.4}$$

K is the coefficient of the vertical eddy viscosity, which is defined by

$$K = l^2 \left\| \frac{\partial \mathbb{V}}{\partial z} \right\|, \tag{4.5}$$

l is the mixing length as a function of Z.

The boundary conditions are: at the ground surface, i.e., $\sigma = 1$ or more precisely $z = z_0$,

$$u = \dot{\sigma} = 0, \tag{4.6}$$

$$K\frac{\partial u}{\partial \sigma} = -C_D |\mathbb{V}| \mu \tag{4.7}$$

and at $\sigma = 0$,

$$\dot{\sigma} = 0. \tag{4.8}$$

The centered time differencing for the "forward" process is written as

(1st step)

$$\hat{u} - u^{\tau-1} = \underbrace{\left[-\left(u \frac{\partial u}{\partial x} + v \frac{\partial u}{\partial y} + \dot{\sigma} \frac{\partial u}{\partial \sigma} \right) + fv - \frac{\partial \phi}{\partial x} \right]^{\tau}}_{F_u^{\tau}} 2\Delta t, \tag{4.9}$$

$$\hat{T} - T^{\tau-1} = \underbrace{\left[-\left(u \frac{\partial T}{\partial x} + v \frac{\partial T}{\partial y} + \dot{\sigma} \frac{\partial T}{\partial \sigma} \right) + \frac{RT\omega}{p_s \sigma C_p} \right]^{\tau}}_{F_T^{\tau}} 2\Delta t, \tag{4.10}$$

where the sufixes τ and $\tau - 1$ are the time levels, Δt is the time step and $\hat{u}$ is the unknown for u, and so is $\hat{T}$.

(2nd step)

$$u^{\tau+1} - \hat{u} = \frac{\partial}{\partial \sigma} \left(K^{\tau} \frac{\partial u^{\tau+1}}{\partial \sigma} \right) \cdot 2\Delta t, \tag{4.11}$$

$$T^{\tau+1} = \hat{T}, \tag{4.12}$$

where

$$K^{\tau} = l^2 \left| \frac{\partial \mathbb{V}^{\tau}}{\partial z} \right|. \tag{4.13}$$

In eq. (4.11), for example, the unknowns are $u^{\tau+1}$ on the left-hand side and $(\partial u/\partial \sigma)^{\tau+1}$ on the right-hand side, so that this constitutes an implicit equation for $u^{\tau+1}$, but it can be solved readily as a simple boundary value problem. In summary, if the variables at time levels $\tau - 1$ and τ are given, those at $\tau + 1$ are obtained in the system of the first and second steps.

The "backward" process is then written as

$$u^{\tau-1} - u^{\tau+1} = -\left[F_u^{\tau} + \frac{\partial}{\partial \sigma} \left(K^{\tau} \frac{\partial u^{\tau+1}}{\partial \sigma} \right) \right] 2\Delta t, \tag{4.14}$$

$$T^{\tau-1} - T^{\tau+1} = -F_T^{\tau}\, 2\,\Delta t. \tag{4.15}$$

In the above equations, if the variables at time levels $\tau + 1$ and τ are given, those at $\tau - 1$ are obtained explicitly by a one-step calculation. Therefore, in this case, the hindcast calculation is simpler. It was proven in a real numerical calculation (10 steps forward, 10 steps backward) that this scheme provides a very good reversible process.

B. The second example includes the dry convective adjustment, surface drag, surface heat flux (land-sea contrast) and radiation, in addition to the physical processes in case A.

The equations are written as

$$\frac{du}{dt} = fv - \frac{\partial \phi}{\partial x} + \frac{\partial \tau_u}{\partial \sigma}, \tag{4.16}$$

$$\frac{dT}{dt} = + \frac{RT\omega}{C_p P_s \sigma} + \frac{\partial \tau_T}{\partial \sigma} + Q_{\text{conv}} + Q_{\text{rad}}, \tag{4.17}$$

where

$$\tau_u = K \frac{\partial u}{\partial \sigma}. \tag{4.18}$$

Q_{conv} and Q_{rad} are the rates of heating due to the dry convective adjustment and long-wave and short-wave radiation, respectively. The dry convective adjustment is included; the vertical temperature distribution is adjusted to be at the dry adiabatic lapse rate whenever hydrostatic instability tends to occur. The effect is expressed by the term Q_{conv} in (4.17).

The boundary conditions are: at $\sigma = 1$,

$$\tau_u = -C_D |\mathbb{V}| u, \tag{4.19}$$

$$\tau_T = C_p C_D |\mathbb{V}| \left[T_s \left(\frac{p_0}{p_s} \right)^{\kappa} - \theta \right], \tag{4.20}$$

C_D is the modified drag coefficient (ρ is multiplied to the conventional one), C_p is the specific heat at the constant pressure, p_0 is 1000 mb, and $\kappa = R/C_p$. The surface temperature T_s over land is determined by the heat balance equation.

$$\sigma T_s^4 + \tau_T - (1 - A)S - F\downarrow = 0, \tag{4.21}$$

where S is the solar radiation reaching the ground surface, A albedo of the surface, $F\downarrow$ downward long-wave radiation absorbed at the soil surface, and σ is the Stefan–Boltzmann constant (not vertical coordinate only in this case). In this equation, τ_T is a function of T_s given by eq. (4.20). T_s is obtained by the Newton–Raphson iterative method. T_s over sea is specified by

$$T_s = T_{\text{sea}}, \tag{4.22}$$

where T_{sea} is known. Other boundary conditions are the same as in case A.

The time differencing for the "forward" process is written as

(1st step)

$$\hat{u} - u^{\tau-1} = [F_u^{\tau}]2\Delta t, \quad (4.23)$$

$$\hat{T} - T^{\tau-1} = [F_T^{\tau} + Q_{rad}^{\tau} + \tau_T^{\tau-1}\delta]2\Delta t, \quad (4.24)$$

where $\delta = 1$ at $\sigma = 1$, and otherwise $\delta = 0$, and

$$\tau_T^{\tau-1} = C_p C_D |V^{\tau}| \left[T_s^{\tau-1} \left(\frac{p_0}{p_s} \right)^{\kappa} - \theta^{\tau-1} \right], \quad (4.25)$$

and $T_s^{\tau-1}$ is solved from (4.21).

(2nd step)

$$u^{\tau+1} - \hat{u} = \frac{\partial}{\partial \sigma} \left(K^{\tau} \frac{\partial u^{\tau+1}}{\partial \sigma} \right) 2\Delta t, \quad (4.26)$$

$$T^{\tau+1} - \hat{T} = Q_{conv}^{\tau+1} 2\Delta t, \quad (4.27)$$

$$\tau_u^{\tau+1} = - C_D |V^{\tau}| u^{\tau+1}. \quad (4.28)$$

In the "forward" calculation, Q_{conv} and Q_{rad} for all layers of the atmosphere are stored every time step, and they will be used in the "backward" phase. The sensible heat flux from the surface is also stored every time step.

The "backward" process is written as

$$u^{\tau-1} - u^{\tau+1} = -\left[Fu^{\tau} + \frac{\partial}{\partial \sigma} \left(K^{\tau} \frac{\partial u^{\tau+1}}{\partial \sigma} \right) \right] 2\Delta t, \quad (4.29)$$

$$T^{\tau-1} - T^{\tau+1} = -[F_T^{\tau} + Q_{rad}^{\tau} + \tau_T^{\tau-1}\delta + Q_{conv}^{\tau+1}]2\Delta t. \quad (4.30)$$

C. The case in which water vapor and the condensation heat are included. In this case, we have

$$\frac{dT}{dt} = \frac{RT\omega}{C_p p_s \sigma} + \frac{\partial \tau_T}{\partial \sigma} + Q_{dry\ conv} + Q_{rad} + LM_{conv\ cond} + LM_{large\ cond} \quad (4.31)$$

instead of (4.17), and also

$$\frac{dq}{dt} = \frac{\partial \tau_q}{\partial \sigma} - M_{conv\ cond} - M_{large\ cond}, \quad (4.32)$$

where q is the mixing ratio of water vapor, M is the rate of depletion of water vapor, $M_{conv\ cond}$ is due to the condensation of cumulus convection and $M_{large\ cond}$ is due to that of large scale condensation. τ_q is the vertical flux of water vapor by turbulence, and τ_q at the surface is given by

$$\tau_q = C_D |V| [q_{sat}(T_s) - q], \quad (4.33)$$

where q_{sat} is the saturation value of q. The surface heat budget equation is modified such that q is included. The finite differencing in this case is similar to the case of B, except that $(Q_{dry\ conv} + Q_{rad} + LM_{conv\ cond} + LM_{large\ cond})$, $(M_{conv\ cond} + M_{large\ cond})$, (τ_T), (τ_q) are stored at each time level.

The reversibility was tested using a 9-level, $N = 40$ general circulation model. The time range of the round trip (which corresponds to half of the "iteration amplitude" in the terminology of Mesinger, 1972, and Temperton, 1973) is 2 h with a time step $\Delta t = 5$ min. The 10 cycles, therefore, corresponds to 40 hours in the total time span. The reversibility is almost perfect, so that it is very hard to detect any difference of height patterns between the 0th cycle and the 10th cycle, for example. In particular, the 1000 mb maps are normally very sensitive to any perturbation, and yet all details in the height fields at the 0th cycle were reproduced in the maps at the 10th cycle. The height fields in the tropics are influenced by the effect of cumulus convection, but this example showed that the reversibility is remarkably good. It is thus concluded that the schemes proposed in this section provide a reasonable approach for reversible calculations. (The authors have noticed that Kurihara (personal communication) also has succeeded in obtaining the reversible process in a similar way.)

4.3. *Time differencing scheme for data assimilation*

Different from the reversible process described above, the forward-backward adjustment introduces additional processes, i.e., the injection of data or the restoration of variables. This process gives rise to a considerable shock to the model solution. As was shown in Miyakoda and Moyer (1968) by linear analysis, the forward-backward process becomes computationally unstable, when some variables are restored every cycle. As a remedy for making the solution converge by damping out high frequency gravity waves, the Euler-backward scheme has been used (Matsuno, 1966; Kurihara, 1965). In particular, Nitta and Hovermale (1969) proposed two effective methods of application of the Euler-backward scheme to the forward-backward processes. Their second method seems to be very efficient in accelerating the adjustment, but requires additional data storage (Okamura (quoted by Grand and Rivas), Temperton, 1973, and Grand and Rivas, 1975, proposed efficient damping schemes as well, which also require additional storage). Since we are going to apply the method for the storage-consuming general circulation model, the second method was avoided, at least, in the present experimental stage.

Taking for example case B in the previous subsection, we apply the version L of Euler-backward scheme in Nitta and Hovermale (1969). Obviously, the reversibility is disturbed by the damping effect of this time differencing. However, when the model solutions are updated, every timestep by the insertion data, the situation is different.

(1st step)

$$\hat{\hat{u}} = u^{\tau} + (F_u^{\tau})\,\Delta t, \tag{4.34}$$

$$\hat{\hat{T}} = T^{\tau} + (F_T^{\tau})\,\Delta t, \tag{4.35}$$

(2nd step)

$$u^{*} = \hat{\hat{u}} + \frac{\partial}{\partial\sigma}\left(K^{\tau}\frac{\partial u^{*}}{\partial\sigma}\right)\Delta t, \tag{4.36}$$

$$T^{*} = \hat{\hat{T}}.$$

(3rd step)

$$\hat{u} = u^{\tau} + (F_u^{*})\,\Delta t, \tag{4.37}$$

$$\hat{T} = T^{\tau} + (F_T^{*} + Q_{\text{rad}} + \tau_T^{\tau}\delta)\Delta t. \tag{4.38}$$

where

$$\tau_u^{\tau} = -C_D\,|V^{\tau}|\,u^{\tau}, \tag{4.39}$$

$$\tau_T^{\tau} = C_p C_D\,|V^{\tau}|\left[T_s^{\tau}\left(\frac{p_0}{p_s}\right)^{\kappa} - \theta^{\tau}\right]. \tag{4.40}$$

(4th step)

$$u^{\tau+1} = \hat{u} + \frac{\partial}{\partial\sigma}\left(K^{\tau}\frac{\partial u^{\tau+1}}{\partial\sigma}\right)\Delta t, \tag{4.41}$$

$$T^{\tau+1} = \hat{T} + Q_{\text{conv}}^{\tau+1}\Delta t. \tag{4.42}$$

Equation (4.42) corresponds to the dry convective adjustment applied to the current temperature distribution in the vertical. After these steps are completed, the data are entered whichever and wherever they are available. Namely, $u^{\tau+1}$, $T^{\tau+1}$ and $p_s^{\tau+1}$ are replaced by the injected data entirely or partially with the appropriate weighting factor. It is also noted that in these processes, Q_{rad}, Q_{conv} and τ_T are stored evei y time step.

The "backward" process is written as

(1st step)

$$u^{*} = u^{\tau+1} - \left[F_u^{\tau+1} + \frac{\partial}{\partial\sigma}\left(K^{\tau+1}\frac{\partial u^{\tau+1}}{\partial\sigma}\right)\right]\Delta t, \tag{4.43}$$

$$T^{*} = T^{\tau+1} - [F_T^{\tau+1}]\Delta t. \tag{4.44}$$

(2nd step)

$$u^{\tau} = u^{\tau+1} - \left[F_T^{*} + \frac{\partial}{\partial\sigma}\left(K^{\tau+1}\frac{\partial u^{\tau+1}}{\partial\sigma}\right)\right]\Delta t, \tag{4.45}$$

$$T^{\tau} = T^{\tau+1} - [F_T^{*}\Delta t + Q_{\text{rad}}^{\tau+1} + \tau_T^{\tau}\delta + (1 - \delta)Q_{\text{conv}}^{\tau+1}]\Delta t. \tag{4.46}$$

After all steps are through, the data of u^{τ}, T^{τ} and p_s^{τ} are replaced by the insertion data if available.

4.4. *Initialization experiments*

The initialization scheme of the back-and-forth iteration described in the previous subsection was applied to a real data case using the 9-level GC model with full physics. Note that non-linear lateral diffusion was also included. The injected data were of the same kind as used in Exper. n of the "forward" adjustment.

The calculation of the adjustment was started at day-1 or day 0 (see Fig. 3), and, in the former case, the forward adjustment proceeded from day-1 to day 0 using the insertion method of Exper. n. When the calculation reaches day 0 this method was switched to the forward-backward adjustment for the time range from -1 h to $+1$ h, where the same data were repeatedly injected in this period. The forward-backward adjustment was cycled more than seven times, and then the calculation was switched to a pure prediction mode. $\overline{\omega^2}$ increased from day-1 to day 0 and then decreased gradually during the back-and-forth iterations. This indicates that the forward-backward adjustment is indeed effective at reducing the noise level. The time

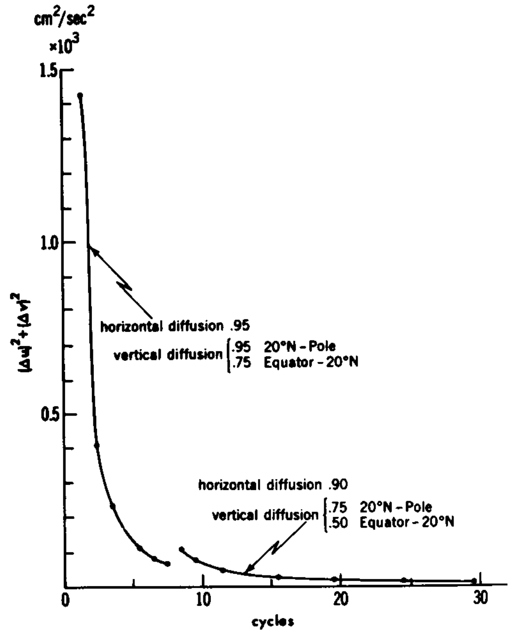

Fig. 13. Convergence in forward-backward adjustment in terms of the difference of wind vector in the successive cycles.

evolution curve of rate of precipitation indicated that the assimilation-prediction transition is smooth.

Concerning the number of iterations required for convergence, Temperton (1973) studied the forward-backward initialization using the shallow water equations, in which iterations corresponding to three days were used. He speculated that if one used the multi-level baroclinic model, the number of iterations must be increased, because the propagation speeds of internal gravity waves are much less than the speed of the external gravity wave.

Haltiner and McCollough (1975) applied the forward-backward adjustment to a multi-level global model, and mentioned that "static balancing, followed by dynamic balancing coupled with a time filter is quite effective". In our study also, this approach was taken, and wind data were inserted. Fig. 13 is the diagram in which a measure of the convergence is plotted versus the number of iteration cycles. The measure is $(\Delta u)^2 + (\Delta v)^2$, the difference of the wind intensity between two successive cycles integrated over the entire volume. In this calculation, we found that the iteration sometimes diverged due to the negative viscosity effect. The poor computational stability in the back and forth iteration was noted by Mesinger (1972). He stated that "friction is beneficial only when applied during the forward part of the last iteration". In our study, we reduced the values of viscosity coefficients slightly in all the backward processes. In the experiment shown in Fig. 13, the ratios of the coefficients between the backward and the forward processes were as follows:

	Horizontal	*Vertical*
1–7 cycles	.95	.95 between 20° N and Pole .75 between Equator and 20° N
8–30 cycles	.90	.75 between 20° N and Pole .50 between Equator and 20° N

As seen in this diagram, the convergence is slow, but 10 cycles (i.e., 40 h, i.e., 1.6 days) yielded practically satisfactory solutions from this standpoint.

However, the convergence of the rate of rainfall is different from that of wind. We made a study on the forward-backward adjustment with Exper. j′ in Table 2, in which the tropical data were inserted and the forward adjustment from −1 day was not included. Fig. 14 depicts the rainfall distribution versus latitude at 9, 20 and 30 cycles, where the amount of condensation was averaged zonally. The diagram also includes the mean rate of condensation in January with the same prediction model (the results were taken from Miyakoda et al., 1972), which indicates the asymptotic values of the rain distribution. It appears that with the j′ system

Table 2. *Experiments of forward-backward adjustment*

Exper.	Data density	Starting day	Remarks
r′	B	−1	
s′	B	−1	Full model (forw.) and simple model (forw.-back.)
t′	B	−1	Dry model (forw.) and dry model (forw.-back.)
g′	C	−1	No data in tropics
h′	C	0	No data in tropics
i′	C	−1	
j′	C	0	

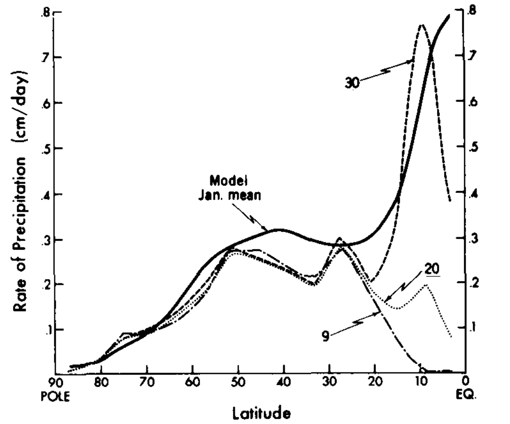

Fig. 14. Latitudinal distribution of rainfall for the cycles of 9, 20 and 30 in forward-backward adjustment.

the convergence of rain in the middle latitudes is very rapid (about 6 h), but that in the tropics is appreciably slow, i.e., 120 h or 5 days.

In this connection, it may be interesting to see the rainfall distribution at day 0 in the forward adjustment of Exper. n. In this experiment, the data were not inserted in the tropics between 10° and the Equator. Consequently, a large shock was given at the latitudes near 15°, the border region between the insertion and the non-insertion areas. The rain has reached an enormous value at these latitudes. When the assimilation of Exper. n was switched to the forecast, the rate of precipitation quickly diminished and at day 4 was near the January average.

In addition to these experiments, we studied the impact of the degree of sophistication in the prediction model upon the quality of the initialization. The question is whether a sophisticated model is really needed to provide a good initialization for the forecasts in the temperate latitudes. For this purpose two additional models were used in conjunction with the test of forward-backward adjustment. One is the *simplest model*, which includes the three-dimensional primitive equations and contains only dry convective adjustment as the subgrid-scale physics and nothing else. The second model is almost the full general circulation model but does not include any effect of water vapor at all, and is referred to as "dry model". In Exper. s′ (see Table 2), the forward adjustment was started at −1 day with the "full model", and at 0 day it was switched to the forward-backward adjustment with the "simple model". After the back-and-forth iteration was cycled 10 times, the calculation proceeded to the prediction with the "full model". In Exper. t′ (Table 2), the forward adjustment was started at −1 day with the "dry model", and at 0 day the forward-backward cycling was started also with the "dry model". After the 10 cycles of back-and-forth iteration, the assimilation was switched to the prediction with the "full model" (Kanamitsu, 1975, also used this type of initialization).

It is rather surprising that the final results of the assimilated maps turned out to be very close to those with the NMC analysis in Fig. 10 so far as the geopotential height field is concerned. This experiment indicates, therefore, that a high degree of sophistication of the prediction model is not completely essential for obtaining the flow fields in the extratropics if a large number of data are inserted (the same thing was experienced by Simmonds, 1976). A pronounced difference is, however, that the precipitation is missing entirely in the initial state in Exper. t′.

4.5. *Various experiments*

The prime is attached to the letters of experiments in Table 2 to discriminate the experiments of the forward-backward adjustment from those of the forward adjustment. In Exper. g′ and h′, the C-network was used for the data insertion, except that no insertion was made in tropics. On the other hand, in Exper. j′ and i′, all data in the C-network, including the tropics, were used. In most of these experiments, the calculations were iterated 10 cycles, except that Exper. j′ was run to 30 cycles.

The skill scores of the forecasts with these initial conditions are the correlation coefficients and the rms error of the geopotential height which are shown in Figs. 15 and 16, respectively, where Exper. q (forward adjustment) and Exper. R are included for the sake of comparison. The results may be summarized as follows: (i) The forecasts with the forward-backward adjustment, Exper. j′, h′ and g′, are clearly better than the forecast with the forward adjustment, Exper. q. This seems to imply that with the forward adjustment the internal balance among various variables is not so satisfactory as that with the forward-backward adjustment. The more perfect balance gives a better forecast than does the imperfect balance. (ii) Exper. j′ and h′ are better than or comparable to Exper. R. (iii) Exper. g′ is inferior to Exper. j′ and h′ except

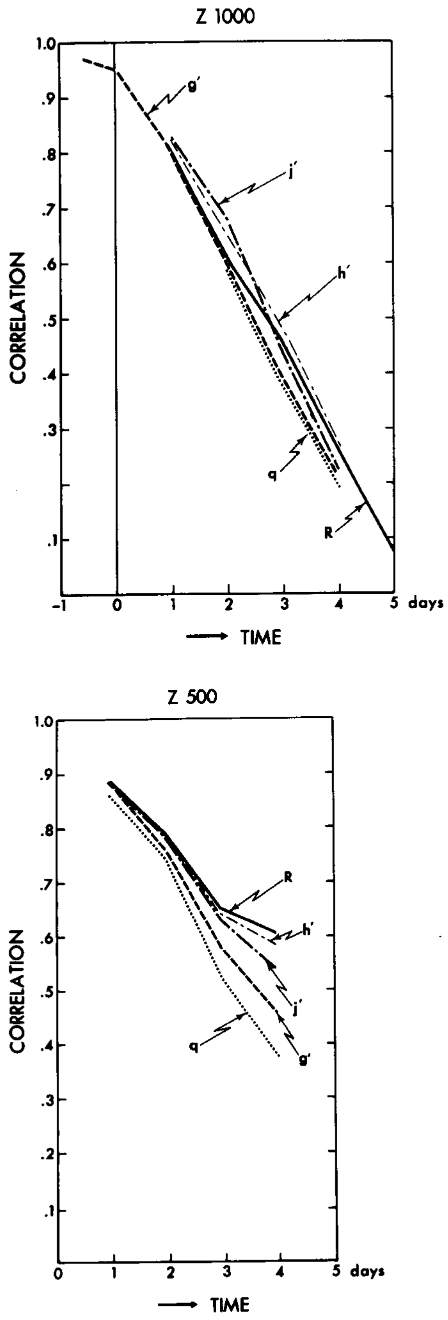

Fig. 15. Correlation coefficients of geopotential height. (a) 1000 mb, (b) 500 mb.

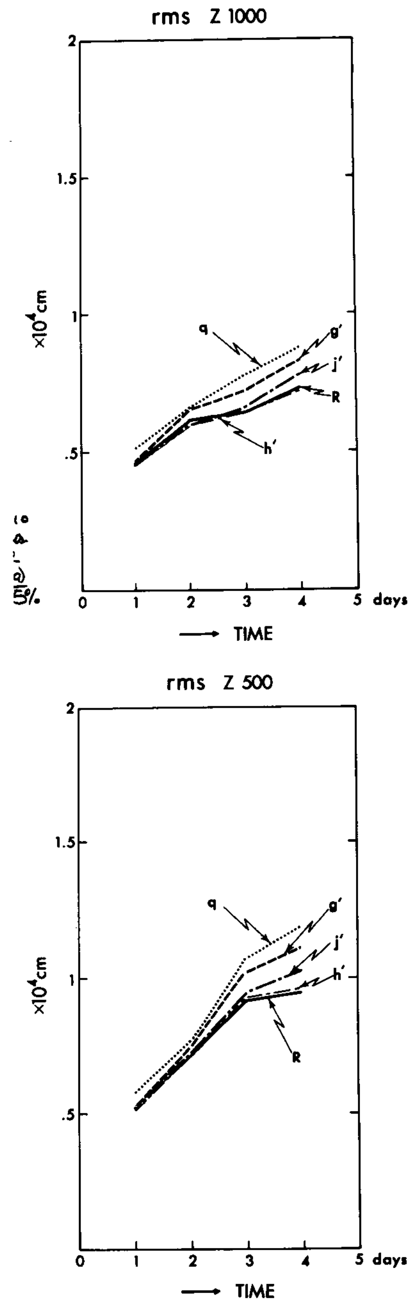

Fig. 16. RMS error of geopotential height (a) 1000 mb, (b) 500 mb.

for the 50 mb geopotential height field (not shown). This means that the combination of forward adjustment and forward-backward adjustment may not be as good as the simple forward-backward adjustment. Apparently, the drawbacks due to the forward adjustment were not entirely eliminated in the back-and-forth process of 10 cycles.

Fig. 17 shows the predicted maps of geopotential height at 4 days with the initial conditions of Exper.

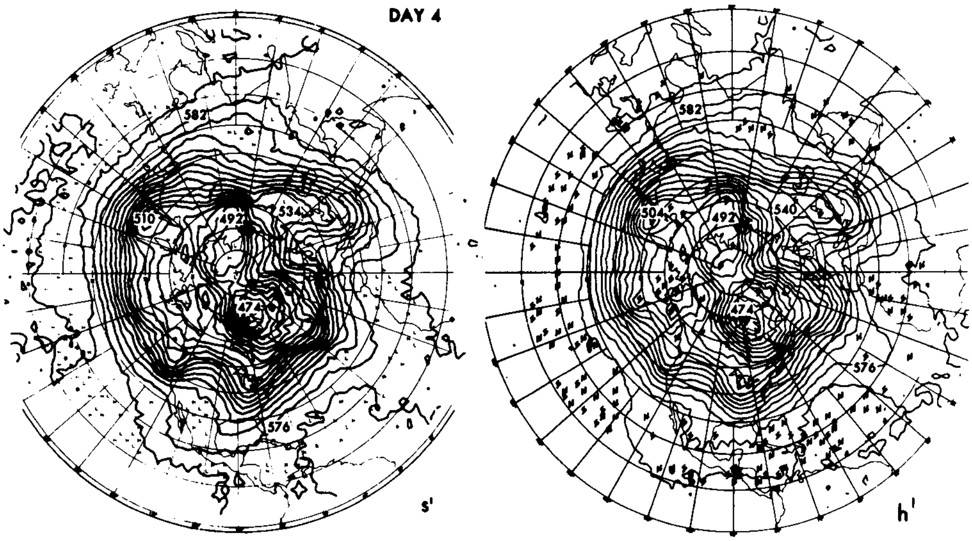

Fig. 17. The 4-day forecasts of the 500 mb geopotential height for Exper. s' and h'. The verification map is in Fig. 12.

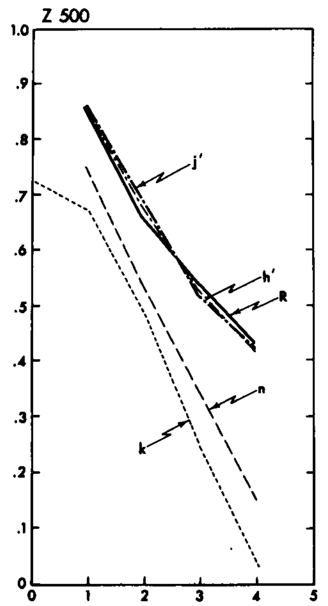

Fig. 18. Correlation coefficients of 500 mb geopotential height for March 1965 case.

s' and h'. Comparing these maps with the results in Fig. 12, one can see that the map of Exper. h' appears as good as Exper. R. A clear difference was not detected.

5. Remarks

A series of similar experiments was conducted for another case, in which data valid at 12 GMT, March 14, 1965, was employed as the initial condition. In this case also, the forecasts with the forward-backward adjustment (Exper. h' and j') were substantially better than those with the forward adjustment (Exper. n and k) (see Fig. 18). It is also true in this case that the forecasts based on the dynamic initialization were slightly better than or comparable to that based on the static initialization, i.e., Exper. R.

Historically speaking, this type of experiment was first carried out by Nitta (1969a, 1969b), who used a 3-level primitive equation model with surface friction and horizontal diffusion. The iterative forward-backward forecast and restoration of mass field every iteration at one time level were applied to the real data, and the relative behavior of the initialization for the forecasts was investigated. In principle, the study in the present paper is exactly the same as Nitta's. Nitta used a limited domain for the test, which evidently created some severe difficulty in obtaining reasonable solutions.

In the present paper we used a more sophisticated model with a larger domain. With all these efforts, however, the dynamical initialization did not give particularly better forecasts than the static initialization. Modelers have recently been aware that the sophistication of the initialization does not necessarily improve the forecast in the extratropics beyond the 3rd day. John Brown (presented at International Symposium on 4-Dimensional Data Analysis for GARP at Princeton, April, 1971) showed that the refined initial condition with the observed wind data in NMC did improve the forecast for 1 or 2 days but did not at the later times so far as the S-1 skill score is concerned. Sundqvist (1976) proposed a scheme of initial balancing on the σ-surface instead of the p-surface, and demonstrated a considerable reduction in gravity waves at the start of the forecast. However, the resulting initial data did not raise the forecast skill. Temperton (1976) mentioned that his "experiments show a rather surprising insensitivity to the precise initial conditions and that the high-frequency oscillation had no appreciable effect on the forecasts of the basic dynamical variables". The problem was studied theoretically by Williamson (1976), using the "model filtering" technique proposed by Dickinson and Williamson (1972), and Williamson concluded that "the gravity waves do not interact significantly with the Rossby waves during the one-day forecast".

It is still true, though, that some initial conditions can give very poor forecasts such as Exper. a, b, k and l. Somewhat imperfect and crude initialization methods (Miyakoda et al., 1971, and Houghton and Washington, 1969) do not give terribly bad forecasts. An example from Washington and Baumhefner (1975) shows that before their method was used to suppress external gravity waves the forecasts were indeed very poor. They show that the surface and 6 km pressure fields were improved by applying their divergence adjustment procedure. Dey and Brown (1976) have pointed out how the numerical method used by Washington and Baumhefner can smooth some of the jet maximums and have suggested an improvement which removes this restriction.

The situation is quite different in the tropical and for meso-scale forecasts, however. Possibly the tropics might need an elaborate initialization scheme including the effect of condensation heat (Kiangi, 1976), and the initial condition for the meso-scale forecasts might also require an accurate condition for the divergent component of wind and the water vapor distribution (Rao and Fishman, 1975). In fact, Kanamitsu (1975) and Krishnamurti et al. (1976) tried to obtain a reasonable dynamic initialization procedure for predictions in the tropics. Haltiner et al. (1976) attempted to employ a simple and economical initialization technique based on the variational principle as a preliminary procedure, and thereafter to use the dynamic initialization as the final refinement.

6. Conclusions

It has been demonstrated that dynamical initialization can give a satisfactory result for the mutually balanced condition of all variables in the model, and the rate of precipitation, vertical velocity, angular momentum etc. can vary smoothly at the initial time and immediately thereafter in the subsequent predictions.

The quality of the forecasts, whose initial conditions were obtained by the forward adjustment technique, varied widely depending on the modes of data injection and assimilation. In general, continuous injection is preferable to intermittent insertion, because the amount of shock generation is less. The use of wind data (even balanced equation wind), in addition to the temperature and surface pressure, is very effective in accelerating the assimilation as well as increasing the accuracy of the resulting condition. It has been well established that mass field injection alone gives a slow rate of assimilation and an inaccurate solution (particularly in the tropics). The injection of higher density data in space generally increases the gravity wave activity but reduces the forecast error overall.

Our test revealed that the forward adjustment has some drawbacks: the final data fields have a high level of noise, and the resulting mass and wind fields lack the detailed structure of the synoptic scale. In this respect, the forward-backward adjustment seems to have better balance among various parameters and to yield better forecasts.

Nevertheless, the overall conclusion is that the forecasts based on the dynamic initialization were only slightly better than or comparable to those based on the static initialization. The original question as to whether the rapid growth of forecast error is due to the defective initial state or the inadequacy of the forecast model has not been answered in this paper. It is conceivable that dynamic initialization could be important for tropical forecasts, because the balanced condition for tropical rain can only be satisfactorily achieved by dynamical initialization.

The knowledge obtained in this study is not only useful for the initialization problem *per se* but also suggests the relative merits of various four-dimensional analyses. In fact, the implementation of four-dimensional analysis of real data during the GATE period in the summer of 1974 (Miyakoda et al., 1976) benefited greatly from this study. A problem for the future is whether or not the forward-backward cycles should be incorporated into the four-dimensional analysis, which so far has been oriented toward the forward adjustment approach.

7. Acknowledgements

The authors wish to acknowledge Drs J. Smagorinsky, R. Asselin, J. Brown, C. T. Gordon, I. Simmonds, H. Sundqvist and W. Washington for their stimulating discussions. They also wish to thank Mr J. Ryan and Ms B. Williams for their assistance.

REFERENCES

Anthes, R. A. 1974. Data assimilation and initialization of hurricane prediction models. *J. Atmos. Sci. 31*, 702–719.

Asselin, R. 1972. Frequency filter for time integrations. *Mon. Weather Rev. 100*, 487–490.

Bengtsson, L. and Gustavsson, N. 1971. An experiment in dynamic analysis. *Tellus 23*, 328–336.

Bengtsson, L. 1975. Four-dimensional assimilation of meteorological observations. *GARP Publication Series No. 15, Joint Organizing Committee, GARP WMO/ICSU.*

Blumen, W. 1975. An analytical view of updating meteorological variables: Part II. Weighted assimilation. *J. Atmos Sci. 32*, 690–697.

Bivins, R. L., Metropolis, N. and Pasta, J. R. 1972. *Nonlinear coupled oscillators: modal equation approach.* Los Alamos Scientific Laboratory, University of California, LA-4934, UC-32, 14 pp.

Bourke, W. 1974. A multi-level spectral model. I. Formulation and hemispheric integrations. *Mon. Weather Rev. 102*, 687–701.

Charney, J., Halem, M. and Jastrow, R. 1969. Use of incomplete historical data to infer the present state of the atmosphere. *J. Atmos. Sci. 26*, 1160–1163.

Davies, H. C. and Turner, R. E. 1977. Dynamical relaxation: a technique for updating prediction models. (To be published in *Quart. J. Roy. Meteor. Soc.*)

Dey, C. and Brown, J. 1976. *Decomposition of windfield on the sphere.* HOAA Tech. Memorandum, NWS, NMC 59 (available at NMC, Washington, D.C., U.S.A.).

Dickinson, R. E. and Williamson, D. L. 1972. Free oscillations of a discrete stratified fluid with application to numerical weather prediction. *J. Atmos. Sci. 29*, 623–640.

Gauntlett, D. and Seaman, R. 1974. Four-dimensional data assimilation experiments in the Southern Hemisphere. *J. Appl. Meteor. 13*, 845–853.

Gordon, C. T., Umscheid, Jr., L. and Miyakoda, K. 1972. Simulation experiments for determining wind data requirements in the tropics. *J. Atmos. Sci. 29*, 1064–1075.

Grant, W. K. F. and de Rivas, E. K. 1977. Initialization procedures for primitive equation models. (Submitted to *Mon. Weather Rev.*)

Haltiner, G. J. 1971. *Numerical weather prediction.* Wiley, New York, 317 pp.

Haltiner, G. J. and McCollough, J. M. 1975. Experiments in the initialization of a global primitive equation model. *J. Appl. Meteor. 14*, 281–288.

Haltiner, G. J., Sasaki, Y. K. and Baker, E. H. 1976. A variational procedure for obtaining global balanced winds. *The GARP Programme on Numerical Experimentation. Rep. 11. Proceedings of the JOC Study Group Conference on Four-Dimensional Data Assimilation.* Paris, 17–21 November, 1975, pp. 198–223.

Hayden, C. M. 1973. Experiments in the four-dimensional assimilation of Nimbus 4 SIRS data. *J. Appl. Meteor. 12*, 425–436.

Houghton, D. and Washington, W. 1969. On global initialization of the primitive equations: Part I. *J. Appl. Meteor. 8*, 726–737.

Kanamitsu, J. 1975. *On numerical prediction over a global tropical belt.* Dept. Meteor. Florida State Univ. Report No. 75-1.

Kiangi, P. M. R., 1976. *A systematic investigation of pressure-wind adjustment laws during initialization and primitive equation prediction over tropical regions.* Ph.D. thesis in University of Nairobi.

Kistler, R. E. and McPherson, R. D. 1975. On the use of a local wind correction technique in four-dimensional data assimilation. *Mon. Weather Rev. 103*, 445–449.

Krishnamurti, T. N., Kanamitsu, M., Godbole, R., Chang, C. B., Carr, F. and Chow, J. H. 1976. Study of monsoon depression II. Dynamical structure. *J. Meteor. Soc. Jap. 54*, 208–225.

Kurihara, Y. 1965. On the use of implicit and iterative methods for the time integration of the wave equation. *Mon. Weather Rev. 93*, 33–46.

Manabe, S., Smagorinsky, J. and Strickler, R. F. 1965. Simulated climatology of a general circulation model with a hydrologic cycle. *Mon. Weather Rev. 93*, 769–798.

Matsuno, T. 1966. Numerical integration of the primitive equations by a simulated backward difference method. *J. Meteor. Soc. Jap. 44*, 76–84.

Mesinger, F. 1972. Computation of the wind by forced adjustment to the height field. *J. Appl. Meteor. 11*, 60–71.

Miyakoda, K. and Moyer, R. W. 1968. A method of initialization for dynamical weather forecasting. *Tellus 20*, 115–128.

Miyakoda, K., Moyer, R. W., Stambler, H., Clarke, R. H. and Strickler, R. F. 1971. A prediction experiment with a global model of the Kurihara-grid. *J. Meteor. Soc. Jap. 49*, Special Issue, 521–536.

Miyakoda, K., Hembree, G. D., Strickler, R. F. and Shulman, I. 1972. Cumulative results of extended forecast experiments, I. Model performance for winter cases. *Mon. Weather Rev. 100*, 836–855.

Miyakoda, K. 1973. Cumulative results of testing a meteorological-mathematical model. The description of the model. *Proceedings of Roy. Irish Academy. 73*, No. 9, 99–130.

Miyakoda, K., Umscheid, L., Lee, D. H., Sirutis, J., Lusen, R. and Pratte, F. 1975. The near-real time global four-dimensional analysis experiment during the GATE period, Part I. *J. Atmos. Sci. 33*, 561–591.

Monin, A. and Obukhov, A. 1959. A note on the general classification of motions in a baroclinic atmosphere. *Tellus 11*, 159–162.

Morel, P., Lefevre, G. and Rabreau, G. 1971. On initialization and non-synoptic data assimilation. *Tellus 23*, 197–206.

Nitta, T. and Hovermale, J. B. 1969. A technique of objective analysis and initialization for the primitive forecast equation. Mon. Weather Rev. 97, 652–658.

Nitta, T. 1969b. Supplement to the experimental forecasts from different initial data. *Meteor. Soc. Jap. 47*, 407–410.

Rao, G. V. and Fishman, J. 1975. An iterative initialization scheme for mesoscale studies. *Tellus 27*, 157–167.

Richtmyer, R. D. and Morton, K. W. 1967. *Difference methods for initial-value problems*. Wiley-Interscience Publishers, Inc., New York, 399 pp.

Rutherford, I. and Asselin, R. 1972. Adjustment of the wind field to geopotential data in a primitive equation model. *J. Atmos. Sci. 29*, 1059–1063.

Sadourny, R. 1972. *Forced geostrophic adjustment in large-scale flows*. Laboratoire de Meteorologie Dynamique, Paris, France.

Simmonds, I. 1976. Data assimilation with a one-level, primitive equation sepctral model. *J. Atmos. Sci. 33*, 1155–1171.

Sundqvist, H. 1976. A consistent way of initialization for PE models using sigma as the vertical coordinate. *The GARP Programme on Numerical Experimentation. Report 11, Proceedings of the JOC Study Group Conf. on 4-Dimensional Data Assimilation.* Paris, 17–21 November, 1975, pp. 181–199.

Talagrand, O. 1972. On the damping of high-frequency motions in four-dimensional assimilation of meteorological data. *J. Atmos. Sci. 29*, 1571–1574.

Temperton, C. 1973. Some experiments in dynamic initialization for a simple primitive equation model. *Quart. J. Roy. Meteor. Soc. 99*, 303–319.

Temperton, C. 1976. Dynamic initialization for barotropic and multi-level models. *Quart. J. Roy. Meteor. Soc. 102*, 297–311.

Washington, A. M. and Baumhefner, D. P. 1975. A method of removing Lamb waves from initial data for primitive equation models. *J. Appl. Meteor. 13*, 114–119.

Williamson, D. and Kasahara, A. 1971. Adaptation of meteorological variables forced by updating. *J. Atmos. Sci. 28*, 1313–1324.

Williamson, D. L. 1976. Normal mode initialization procedure applied to forecasts with the global shallow water equations. *Mon. Weather Rev. 104*, 195–206.

Winninghoff, F. J. 1973. Note on a simple, restorative-iterative procedure for initialization of a global forecast model. *Mon. Weather Rev. 101*, 79–84.

ИНИЦИАЛИЗАЦИЯ С МЕТОДОМ УСВОЕНИЯ ДАННЫХ

Для модели общей циркуляции оцениваются начальные условия, генерируемые методом усвоения данных. При использовании реальных данных, производимых объективным анализом в Национальном метеорологическом центре проверялись два типа динамической инициализации, именно, "опережающее приспособление" и "опережающе-запаздывающее прспособдение". Степень сбалансированности в начальных условиях проверялся в терминах гладкости в развитии величины осадков, момента количества движения и кинетической энергии для начального периода прогноза. Однако качество инициализации оценивалось качеством последующего прогноза. Для опережающего приспособления изучались различные типы схем ввода данных в прогноз с оценкой величин скачков в значениях полей и степени достоверности вводимых данных. В осуществлении опережающе-запаздывающего приспособления имеется трудная задача построения обратимого алгоритма. Представлен приближенный метод поддержания обратимости в системе, где есть диссипация кинетической энергии, радиация и выделение скрытой теплоты. В дополнение обсуждается вопрос, какие физиуеские процессы следует учитывать при опережающе-запаздывающей инициализации. Найдено, что динамическая инициализация, использующая опережающе-запаздывающее усвоение данных дает прогнозы, которые в некоторых отношениях лучше прогнозов с данными, полученными путем статической или обычной инициализации. Однако для опережающего усвоения данных прогнозы хуже, чем при статической инициализации.